DEFORMATION ANALYSIS FOR MOTORCYCLE HELMETS

A GILCHRIST & N J MILLS
School of Metallurgy and Materials,
The University of Birmingham, Birmingham, B15 2TT, UK.

ABSTRACT- Experimental measurements have been made of the shell deformation during the impact of a motorcycle helmet, and the compressive stress-strain relationship of the foam liner. The information was used to construct a computer model of the performance of helmets, that allows the effects of different shell materials, and of different foam densities, to be predicted. The main events in the deformation of an impacted helmet were identified and the optimisation of the design for particular types of impact is discussed.

1 INTRODUCTION

The authors[1] made a preliminary analysis of the performance of motorcycle helmets in 1988. Subsequently we have made measurements both of the foam impact performance[2] and of the helmet shell deformation[3]. This has allowed a re-examination of the modelling of the overall helmet performance. The reason for such modelling is to assist in the design of improved helmets, and to be able to analyse acceleration-time traces, collected from tests on many designs of helmets, in terms of the performance of the components. Helmet designers empirically select the density and thickness of the polystyrene foam to meet the impact tests in the standard, which are at one velocity (5 to 8 m s^{-1} depending on the standard) onto rigid flat and convex anvils, with the impact sites not including the front edge of the shell[4]. The shell thickness is determined by the need to pass a penetration test, in which a conical steel indenter with a 90 J impact energy(in BS 6658, or 30 J in prEN 398[5]) must not penetrate to touch the headform. In real crashes the impact are at a range of velocities; the sites struck are mainly the front and sides of fullface helmets[6]; the objects struck are mainly flat and rigid[7].

It is possible to carry out helmet tests over a range of impact velocities, onto different types of object, with a range of impact sites, but this is an expensive method of assessing the overall performance of a helmet. An understanding of the main deformation mechanisms and the causes of mechanical vibration in an impact would allow the test programme to be reduced, and the limitations of each design of helmet to be evaluated. For a direct impact onto an immovable anvil a helmet design will only keep the peak head acceleration below the biomechanical limit for impact velocities below some limit. The value of this critical velocity depends on the impact site and the shape of the object struck.

A ring-element computer model, with axial symmetry , was used to analyse impacts on the crown of motorcycle helmets[8]. This model did not consider the force oscillations due to the acceleration of the helmet components. It will be shown later that force oscillations are significant in helmet impacts at velocities of 2 to 10 ms^{-1}. The simple model presented here is a first attempt at covering all the significant phenomena in a helmet impact.

2 MODELLING

2.1 Components of the helmet

The main impact absorbing component is the foam liner, which is usually moulded from polystyrene beads. Polystyrene foam has a low density, is economic to mould, and has good one-impact energy absorption. There is comfort-foam inside the helmet to keep out draughts, and to allow a limited range of helmet sizes to fit a great range of head sizes. Helmet shells are either injection moulded from ABS(Acrylonitrile Butadiene Styrene copolymer) or rubber-toughened polycarbonate, or moulded from polyester thermoset resin reinforced with glass fibre (GRP). Table 1 summarises the main deformation mechanisms in a helmet. The details of the data for each of these will be given, and these four mechanisms will appear as the four spring/dashpot elements in the model.

Table 1 Helmet components and data for their impact behaviour

Component	Data source	Data treatment
Polystyrene foam crushing	impact tests on rectangular blocks	curve fit with eqn(1). Integrate across contact area
comfort foam compression	impact tests on rectangular blocks	curve fit with eqn(9).
shell deformation	impacts on shells with accelerometers at sides	interpret force-deflection data to give loading stiffness & force to buckle/delaminate
elastic deformation of polystyrene foam	force difference between head and striker	measure resonant frequency and infer stiffness

2.2 Structure of the model

Fig 1a shows the load paths that exist between the head and the object struck, and Fig 1b the model used. There are 4 masses involved

m_1 of the steel striker or anvil. This can be infinite if it represents the road surface.

m_2 of the helmet shell

m_3 of the helmet liner foam

m_4 of the headform (5 kg in BS 6658, 3.1 to 6.1 kg in prEN 398).

In Fig 1b the equivalent paths through the model are shown. The convention is used that horizontal members remain horizontal when the springs or dashpots deform, so single position variables x_1 to x_4 can be allocated to the masses m_1 to m_4. The variables x_3 and x_4 do not represent single locations on the inner surface of the liner and the headform, but the x component of the general point on these constant shape surfaces. Hence the difference $x_3 - x_4$ represents the vertical component of the gap between the liner and the headform. The masses are only permitted to move along the vertical x axis, so the model cannot simulate the rotation of a helmet on a headform.

The loading paths are either through the crushed foam liner, or through the outer regions of the shell and the uncrushed liner, to the comfort foam, then to the headform. Load path 1 involves the bending of the shell(parameters k_1 and n_1) in series with the elastic deformation of the liner(parameters k_2 and n_2). Load path 2 contains the force deflection relationship of the crushed polystyrene foam, and that of the comfort foam(parameters k_3 and n_3). The parallel connection of load paths 1 and 2 implies that the flat or hemispherical anvil deforms the polystyrene foam from the outside(Fig 2a). The area of crushed polystyrene is too small to allow the rigid headform to penetrate the inner surface of the liner. Consequently the position variable x_3 for the inner surface of the liner is the same for load paths 1 and 2. Experimental evidence[3] shows that there is considerable crushing of the inside of the liner by rigid metal headforms, especially for impacts with rigid flat surfaces. This is due to the lack of an exact fit between the inside of the liner and the surface of the headform. In real life the deformable heads of motorcyclists make a good fit to the inside of their helmet liners, and this interior crushing mechanism does not occur. Consequently the model was made to reflect the real world situation rather than the artificial conditions of helmet testing.

2.3 Crushing of the polystyrene foam

The compressive stress strain behaviour of foams under impact conditions has been measured [9]. For polystyrene foam the loading parts of different impact energy stress-strain curves superimpose to form a mastercurve. We used a gas pressure hardening expression [10] to curve fit the stress strain mastercurve of polystyrene foams.

$$\sigma = \sigma_o + \frac{p_o \varepsilon}{1 - \varepsilon - D} \qquad (1)$$

ε is the compressive strain and σ is the stress, while σ_0 is the initial yield stress of the foam. D

is the relative density of the foam compared with that of the bulk polymer. p_0 should be the pressure of the gas in the cells in the undeformed foam(1 bar) but it is used as a disposable constant for the strain hardening of the foam. For a polystyrene foam of relative density D there are two constants that describe the compressive loading stress strain curve(for D = 0.030, σ_0 = 0.315 MNm^{-2} and p_0 = 0.10 MNm^{-2}). The relationship between σ_0 and D was found experimentally to be

$$\sigma_0 \cong \sigma_p D^{1.5} \qquad (2)$$

where σ_p is the yield stress of the solid polymer. The constant $p_0 \cong 0.1$ MNm^{-2} for relative densities D < 0.035, then it rises towards 0.2 MNm^{-2} at higher densities. For the initial small strains less than 6% an elastic loading expression was used that rises to the yield stress σ_0 of equation (1).

In order to calculate the force(F)-deformation(x) relationship for the foam in the crushed contact area of foam we must know the geometry of the headform and of the object struck by the helmet. The approximation used is that the headform is locally spherical and rigid. The object struck is taken either to be flat and rigid, or a rigid hemispherical anvil of radius R_a = 50 mm. For the impact on the flat anvil the geometrical parameter of importance is R_h, the local radius of curvature of the helmet exterior. In [2] we used the approximation that the yield stress σ_y of the foam was a constant and showed that the contact force F was

$$F \cong 2 \pi R_h \sigma_y x \qquad (3)$$

where x is the central deflection of the foam. This approximation assumes that the helmet shell is not stiff enough to increase the contact area above that for a shell-less helmet. For an impact on a hemispherical anvil of radius R_a, the parameter R_h in equation (3) should be replaced by R where

$$\frac{1}{R} = \frac{1}{R_a} + \frac{1}{R_h} \qquad (4)$$

This equation predicts that for R_a = 50 and R_h =140 mm then R = 37 mm. Experimental studies of the contact area[11] show that the 4 mm thick ABS shell of a motorcycle helmet considerably increases the contact area for impacts with hemispherical anvils. Hence in the later modelling the value of R was set at 70 mm.

We need to allow for the strain hardening of the foam. Figure 2b shows the pressure distribution across the contact area. The total contact force is the sum of the forces on 20 concentric annuli, with a different compressive strain on each. This gives a good approximation to the force integral, using

$$F = \sum_{i=1}^{20} \sigma_i \, 2\pi r_i \, \Delta r \qquad (5)$$

Fig 3 shows the predicted contact force as a function of the deflection value x at the centre of the contact area for a 25 mm thickness of polystyrene foam of density 56 kg m^{-3}(σ_0 = 0.73 MNm^{-2} and p_0 = 0.156 MNm^{-2}) in a helmet of shell radius 140 mm. The force on the contact area rises nearly linearly with the central compression, because the integral is dominated by forces on the outer, low strain, annuli. When the central strain rises to > 96% there will be the equivalent of metal to metal contact between the headform and the anvil. A term was placed in the analysis to allow for this eventuality, which will cause the head acceleration to exceed 500g. If the liner deflection at the centre of the contact area falls during the impact the total force is assumed to fall along a line of slope 5 kN/mm. Any reloading will also follow this line until the curve in Fig 3 is met again.

2.4 Shell deformation

To measure the shell deformation the helmet was supported on a rigid aluminium headform, which is mounted via a load cell to a massive steel plate. Two miniature accelerometers were fixed to the exterior of the shell, at positions remote from the impact site, with their axes vertical. The 5 kg striker is guided by two cables so that it can only move along a vertical axis, and an accelerometer is mounted on the top of the striker. The mean of the left and right shell accelerations is subtracted from the acceleration of the striker and the resulting quantity integrated twice with respect to time to calculate the deformation of the contact point relative to the remote parts of the shell.

The results of the tests(table 2) show that thermoplastic helmet shells are less stiff than GRP ones and they rebound more. The radius of curvature of the shell at the impact point varied from 120 mm in the left to right direction to 140 mm in the fore and aft direction. The centre of the impact was 120 mm above the top of the visor aperture. Buckling of the thermoplastic shells was only observed for the impacts with a hemispherical anvil. To interpret the loading slope data in table 2 we assumed that the shell is loaded while it is accelerating away from the striker, and the liner is not in firm contact with the headform. Hence the loading slopes in table 2 are the initial stiffnesses k_{1a} of the shells. The values are very close to the static stiffnesses measured on sections of shells supported at the rim on a steel plate[2].

Table 2 Data from the loading curves for shell deformation

Helmet	Shell Material	striker	site	loading curve slope N/mm	buckle(B) or delamination(D) force kN
UK ff	ABS	hemi	front	690	3.0 B
UK ff	ABS	flat	front	700	none < 9
Italy ff	glass fibre	hemi	front	1350	3.5 D
Italy ff	glass fibre	flat	front	2250	none < 10

Helmet style:- ff - fullface.

The form of the experimental force-deformation relation is compared in Fig 4 with the idealisation used in the model. On loading the slope of the graph falls from the initial high value $k_{1a} \cong 700$ N/mm to the lower post-buckled value $k_{1b} \cong 200$ N/mm when the force exceeds the buckle force F_b. If unloading occurs it is at the high slope k_{1a} until the force has fallen by F_b. On subsequent reloading the force increases at the high slope k_{1a} until it rejoins the line of the earlier loading. If there is complete unloading to a zero deflection any new loading will follow the path of the initial loading. The value of the dashpot constant n_1 was chosen so that the ratio n_1 / k_1 is 0.2 ms; this ensures that there is a realistic amount of hysteresis in the loading/unloading sequence in the absence of buckling.

The buckling process does not damage the thermoplastic, rather it is an example of high strain(up to 10% on the surface) single fatigue cycle. However when GRP shells hit a hemispherical anvil there is delamination between layers of the glass matt/roving/cloth reinforcement, which means that on reloading the stiffness of the shell will have decreased.

2.5 Compression and shear of the elastic region of the polystyrene foam

The Young's modulus of closed cell foams is given to a good approximation by

$$E = E_p \, C \, D^{1.5} \qquad (6)$$

where the constant C is equal to 1.0, E_p is the modulus of the solid polymer (3.0 $GNMm^{-2}$ for polystyrene) and D is the relative density of the foam compared with the bulk polymer[9]. This part of the model relies on experimental data for the difference between the headform force F_h and the striker force F_s versus time. When the crown of a Jet style helmet, containing a polystyrene foam of density 60 kg m^{-3}, was impacted the difference $F_h - F_s$ was found to oscillate at a frequency of 400 Hz[9].

As the resonant angular frequency ω of a single spring, spring constant k and mass m is

$$\omega = \sqrt{\frac{k}{m}} \tag{7}$$

then for a shell mass of 0.6 kg the spring constant must be 4.0×10^6 N m^{-1}. This value was used for the stiffness k_2 of a foam liner of density 56 kg m^{-3}. The compressive spring constant k of a block of foam of area A, thickness t and Young's modulus E is

$$k = \frac{EA}{t} \tag{8}$$

The liner foam is loaded in a mixture of shear and compression, but as there is a similar relationship to eqn(8) for the shear spring constant, equations (6) and (8) lead to the rule that the liner stiffness k_2 is proportional to the square of the relative density of the foam. Hence the k values are scaled from that for the 56 kg m^{-3} density foam. There is a viscous dashpot in parallel with the spring and the value of the dashpot constant n_2 is chosen so that the retardation time $n_2/k_2 = 0.25$ ms.

2.6 Compression of the open-cell comfort foam.

The comfort foams used are polyurethane or PVC foams often faced with a cloth layer. The uncompressed foam thickness of ~ 5 mm is not a good estimate of the gap between the inside of the polystyrene liner and the skull of the wearer, because the foam is compressed at local high points on the head while there were air gaps at other locations. It was difficult to measure the impact stresses on comfort foams at low strains because the compressive stresses were orders of magnitude below those for polystyrene foam, and the accelerometer on the falling striker test rig was insufficiently sensitive. Therefore the initial part of the stress strain curve was measured under slow speed compression tests on an Instron mechanical testing machine. Fig 5 shows that the force rises rapidly above a strain of 80%. For the modelling the contact area was taken as being constant and equivalent to a disc of radius 75 mm. The experimental curve was fitted by

$$F_{34} = k_3(x_4 - x_3) + n_3(V_4 - V_3) \qquad \text{if } e < 0.6 \tag{9}$$

and if the strain ε in the foam exceeds 0.6, the factor k_3 is multiplied by

$$\exp(40(\varepsilon - 0.6)^2)$$

to approximate the bottoming out of the foam. There is a viscous dashpot in parallel with the spring in the model, and the ratio $n_3 / k_3 = 1$ ms. This produces a significant viscoelastic effect when the loading velocity is 5 ms^{-1} (Fig 5). The constant n_3 may be unrealistically large for the stress strain behaviour of polyurethane foam, but such a value was required to prevent overlarge force oscillations when the liner hits the headform in the modelling process.

3 THE COMPUTER MODEL

3.1 Basis of the model

The model can cope with the two main types of helmet tests, those with a fixed headform and a moving striker, and those with a fixed anvil onto which the helmetted headform falls. In the core of the programme the following sequence is repeated at time interval of 2 μs

i) the old positions x_i and velocities V_i of the 4 masses are used
ii) The forces acting on the masses are calculated using the constants for the elements. For instance the force F_{23} acting between masses 2 and 3 is calculated using

$$F_{23} = k_2(x_3 - x_2) + n_2(V_3 - V_2) \tag{10}$$

The calculation of the forces for shell bending and for the crushing of the polystyrene

foam is more complex because it depends on whether there has been any unloading (sections 2.3 and 2.4). The forces on masses m_1 and m_4 are not allowed to be negative so that the helmet can move freely away from the headform and from the anvil.

iii) the new accelerations of the masses are calculated using Newton's 2nd law. For instance

$$a_1 = \frac{F_{12} + F_{13} + F_{14}}{m_1} + g_1 \qquad (11)$$

The term g_1 is equal to 9.81 ms^{-1} if the striker is freely falling or zero if the anvil is fixed.

iv) The new velocities of the masses are calculated after a time interval Δt from the old velocities using

$$V_{i,\,new} = V_{i,\,old} + 0.5(a_{i,\,old} + a_{i,\,new})\,\Delta t \qquad (12)$$

v) The new positions of the masses are calculated by a similar numerical integration of the velocities over the time interval Δt.

The output of the model can be shown in various ways:- as the forces on one of the masses as a function of time, as the deflection of all or part of the helmet, or as the force as a function of the energy input to the helmet. It is possible to model the effects of second impacts by reusing the maximum polystyrene liner deflections used in the simulation of the first impact.

3.2 Model Predictions

The deformations of the helmet components versus time are shown in Fig 6 for an impact of a flat striker on a region of the shell with a radius of curvature of 140 mm. The comfort foam compression(x_3 - x_4) rises rapidly to more than 90% of the comfort foam thickness in the early stages of the impact event. The striker force begins to rise to an initial peak during the comfort foam compression. The implication is that the comfort foam is too soft to impede the acceleration of the complete helmet away from the striker. Once the comfort foam is highly compressed it becomes very stiff and plays very little part in the subsequent events.

The elastic bending of the polystyrene liner(x_3 - x_2) initially moves in a negative direction while the comfort foam is being compressed. This is interpreted as the inner surface of the liner below the impact site approaching the headform, while the outer regions of the liner have not moved. At this stage the elastic part of the liner has flattened in the region surrounding the impact site. The part of the liner-bending curve after 2 ms shows a large positive peak followed by damped oscillations. At the peak the outer parts of the liner are moving more than the contact region, so the outer parts of the liner are becoming more curved and/or shearing. Since the sides of the liner can move without coming into contact with the headform, this motion is only limited by the bending/shear stiffness of the liner. Therefore the shell mass m_3 can oscillate on the elastic part of the liner.

The liner crush(x_3 - x_1) increases to a peak of 5 mm after 1 ms; this may represent the crushing of the outer layers of the foam under the striker, because the local pressure on the comfort foam side of the liner is below the yield stress of the polystyrene at this stage. The liner crush then rises to a peak of 12 mm after 4 ms. In this test with 123 J of impact energy the maximum in the liner compression at the centre of the contact area is only ~ 50% of the 25 mm liner thickness. In a falling headform test at the same impact velocity of 7 ms^{-1} the impact energy would be ~ 20% higher because of the extra 1 kg mass of the helmet, and therefore the maximum liner compression would be ~ 20% higher. The shell bending (x_2 - x_1) curve has the same general shape as the liner compression, and is not shown in the figure to avoid confusion.

Fig. 7a shows the predicted variation of the striker force and the headform force with time. The force on the headform shows two distinct peaks, the first being due to the impact of the inside of the rapidly moving helmet with the headform. The first peak is the higher in this test, which suggests that a change in the characteristic of the comfort foam would be able to reduce the peak acceleration of the whole test. A stiffer comfort foam would not allow such a sudden impact of the interior of the polystyrene foam on the headform. The predicted forces exceed the BS 6658 test criteria, whereas the real helmet passed the BS6658 test because the

headform partly penetrated the liner from the inside. Comparison with the equivalent graphs of the component deformation(Fig 6) shows that the peak A in the striker force occurs while the comfort foam is being compressed and the helmet is accelerating away from the anvil. The headform force does not rise rapidly to peak B until this process is complete. The relative magnitude of the peaks can be changed by altering the comfort foam thickness. The subsequent minimum in the headform force at C is due to the oscillation in the value of the elastic liner bending. The second peak at D is again a result in the large scale oscillation of the mass of the helmet shell on the elastic part of the liner. The peak in the striker force at E is smaller than either of the peaks in the headform force and it occurs close the point where the liner compression is a maximum. In other simulations the striker/ anvil force maximum is higher than the headform force by amount up to 20%, which shows why it is necessary to measure the headform force in helmet test standards.

Fig 7b shows an experimental result for an equal energy impact on the crown of a Jet style helmet. The same features are shown as in Fig 7a but the magnitudes of the peaks are smaller. This is due to there being some extra crushing of the polystyrene liner from the inside by the headform. The amount of filtering of the signal for the striker force is less than that for the headform trace, so the slight ringing of the striker trace in the initial peak should be ignored.

3.3 The effect of the impact velocity on the helmet performance

The model can be used to evaluate a certain design over a range of impact conditions. Fig 8a shows how the peak headform force in a falling headform test onto a flat surface increases with the impact velocity until it reaches the failure limit of 15 kN(equivalent to the 300 g acceleration limit in BS 6658:1985, for headform mass 5 kg). The peak force is a nearly linear function of the velocity, and the force limit is reached at a velocity of 6 ms^{-1}. It can be seen from the superimposed graph of the peak liner crush that the force limit is reached when the liner crush is only 11 mm; this is only 44% of the liner thickness and shows that the 56 kg m^{-3} liner density is too high to be optimal for this test. Fig 8b shows the performance of the same design for impacts into a hemispherical anvil; in this case the 15 kN limit is not reached until the velocity is 8.8 ms^{-1} and the liner is 98% crushed. For any higher velocities the headform force rises immediately to injurious levels. In this case the foam density is optimal. There are impact sites on the front of the helmet where the average radius of curvature of the shell is ~130 mm (the 140 mm value used in these calculations is close to the median value of the shell), and where the shell stiffness is less due to the proximity of a free edge. For these sites the slopes of the predicted maximum headform force versus velocity graphs will be less, which will mean that polystyrene foam of 56 kg m^{-3} density will be of lower than optimal yield stress for the hemispherical impact and nearer to optimal for the flat impact. Conversely at the side of the helmet the average radius of curvature is 170 mm which means that the high density foam is even less ideal for impacts into a flat surface.

If a polystyrene foam of low 32 kg m^{-3} density is used in the simulated impacts into a flat anvil it is possible to reduce the peak headform accelerations by 27% over the range of impact velocities up to 8 ms^{-1}, and to increase the velocity to cause a peak headform force of 15 kN by 25%, compared with the results for a foam of density of 56 kg m^{-3}. When the high loading stiffnesses for GRP shells from table 2 were used in the simulations, the effect shown in Fig 8a, of the foam yield stress being too high to optimise impacts with a flat surface, was larger. As GRP shells are of varied construction, and there are differences in thickness from point to point on the same shell, it was felt to be more useful to present results for the more consistent thermoplastic shells.

3.4 The performance in second impacts

The predicted results of second impacts in the test standards are instructive as they reveal which impact is critical in the design. In BS 6658 there is a second impact at a reduced velocity using the same anvil at exactly the same site. The velocities specified differ according to the grade of the helmet(A or B) and the anvil shape. We have simulated the impact of type A helmets onto a hemispherical anvil, with successive velocities of 7 and 5 ms^{-1}. It was found that the second impact, which has 51% of the kinetic energy of the first, does not cause a 56 kg m^{-3} density liner to deform to any greater strain than the 70% in the first impact. Hence the first

impact is the critical one. It would only be possible for the second impact to be critical if the test conditions in the first impact caused the liner strain to be close to 100%.

In the prEN 398 impact tests there is a first impact at 7 ms^{-1} onto a flat anvil followed by a second impact, at a site 15 mm away from the first, at 6 ms^{-1} onto a hemispherical anvil. The spacing of the impact sites is insufficient for the second impact to avoid the damage from the first impact. It is difficult in the modelling to allow for the partial overlap of the impact sites, so we have assumed that the second impact is at the same site. Fig 9 shows the force on the anvil versus the total deflection of the liner and comfort foams. The second impact has 73% of the kinetic energy of the first impact and it causes the total deflection to increase by 4 mm. It is necessary to keep some liner crush distance in reserve in the first impact, for the critical second test to be passed. A high density foam must thus be used for the helmet to pass the two impact tests. The first impact must not cause a liner peak strain in excess of 80% otherwise there will not be reserve energy absorption capacity for the second impact. There is no statistical evidence[12] that multiple impacts occur on the same spot in crashes - there is evidence of multiple impacts but these involve different objects and, as there is always some rotation of the motorcyclist's head, the probability of two major impacts on the same site is small. The damaged area for a major impact is ~ 100 mm diameter, which is 5 % of the total protected area on a helmet shell. If the second impact is at a randomly selected site on the shell then the probability that its centre is within 80 mm of the centre of the first impact is only ~5 %. We conclude that the second impact test is unnecessary, and that it can lead to the use of foams of higher than optimal yield stress for the first impact. If the second impact is performed to reject helmets where the shell fractures in the first impact, then there are other ways of achieving this.

3.5 The impact site and the shape of the object struck

Current designs of motorcycle helmets are not optimised for impacts on to rigid flat surfaces, when the impact site is away from the front edge of the helmet. One reason for the use of high foam densities is that there are also impacts onto hemispherical anvils, and there are impact sites towards the front of the helmet where the shell is less stiff than for the site used in the model. It is necessary for the helmet to pass all the tests, hence the density used must be the best compromise. In some helmets the foam in the crown of helmets has been modified either by reducing the area by drilling holes, or by using inserts of lower yield stress foam. The design of helmets is nearly optimal for the range of impact tests in the British Standard, so it is necessary to review the tests in the standard.

The requirement for a penetration test in the motorcycle helmet standards has lead to the shells being relatively thick. This is noticeable by comparing the designs of bicycle helmets and horse riding helmets where the relevant standards do not contain penetration tests. There are many designs of bicycle helmet which do not have a shell, and it is common with the BS 4472 Jockey skull caps to have a very thin(< 1 mm) fibreglass shell which delaminates easily in an impact. The high energy penetration test in BS 6658 is particularly severe and it has lead to GRP shells that do not delaminate for high energy impacts into a flat rigid surface. Such helmets pass the BS impact tests but our measurements of shell deformation[3] show that this is partly due to the rigid headform penetrating the foam liner from the inside, which is not observed with helmets from crashes. The surveys by Pedder[12] show that shell penetration by sharp objects is extremely rare, so we feel that the penetration test should be dropped altogether. It is understood that a meeting of the 'Experts in Passive Safety' of the Inland Transport Committee of the EEC in 1992 was in favour of deleting the penetration test and the requirement for a second impact from the United Nations Regulation 22(the standard which is the basis for prEN 398).

3.6 Limitations in the modelling

The main limitation of the one- dimensional model is that the stiffnesses of the shell and the elastic part of the liner cannot be calculated from their shapes, dimensions and material properties; to do this would require finite element analysis. The details of how the components of the model are connected affect the simulation. It is an approximation that the inner surface shape of the liner does not change; in reality the liner will bend elastically when the helmet first contacts the striker, before the comfort foam is fully compressed. This means that the predicted through-thickness liner crushing in the first 1 ms of the impact is unrealistic.

There need to be more measurements of the impact response of comfort foams to confirm the high level of damping assumed in the model. The general level of viscoelastic damping in the model is now similar to that observed in helmet impact traces. If the comfort foam damping parameter is reduced by a factor of 10 then there are predicted to be high frequency force oscillations when the comfort foam bottoms out and the liner interior impacts the headform. There is now greater confidence that the model is valid, and the predictions of the performance of helmets are reliable. If the foam density is varied, the relationships between the parameters in equation (1) and the density can be used to optimise the helmet design for a certain shell and impact test conditions.

REFERENCES

1 N.J. MILLS, A. GILCHRIST & F.J. ROWLAND, Mathematical modelling of the effectiveness of helmet in head protection, *IRCOBI Conference*, 215-226, Bergisch Gladbach, W Germany, (1988)

2 N.J. MILLS & A. GILCHRIST, The effectiveness of foams in bicycle and motorcycle helmets, *Accident Analysis and Prevention,* **23**, 153-63, (1991)

3. N.J. MILLS & A. GILCHRIST, Motorcycle helmet shell optimisation, *Proc. Association for Advancement of Automotive Medicine conference*, 149-162, Portland, Oregon, (1992).

4. BS 6658:1985, Protective helmets for vehicle users, British Standards Institution, London.

5. prEN 398, Protective helmets for drivers and passengers of motorcycles and mopeds, *Comite European de Normalisation,* DIN, Berlin, (1991).

6. D. OTTE, P. JESSL & E.G. SUREN, Impact points and resultant injuries to the head of motorcyclists...., *IRCOBI conference*, 47-64 , Delft, (1984)

7. H. VALLEE et al, The fracturing of helmet shells, *IRCOBI conference*, 99-109, Delft, (1984).

8. H. KOSTNER & U.W. STOCKER, Improvements of the protective effects of motorcycle helmets based on a mathematical approach, *IRCOBI conference*, 195-213, Bergisch Gladbach, Germany, (1988).

9. A.GALE & N. J. MILLS, Effect of polystyrene foam density on motorcycle helmet shock absorption, *Plastics & Rubber Processing & Applic*, **5**, 101-108, (1985).

10. L. GIBSON & M.J. ASHBY, *Cellular solids*, Pergamon Press, Oxford, (1988).

11. S. CHANDLER, A. GILCHRIST & N.J. MILLS, Motorcycle helmet load spreading performance for impacts into rigid and deformable objects, *IRCOBI conference.*, Berlin, 249-261, (1991).

12. J. B. PEDDER, Ph D thesis, University of Birmingham, (1993).

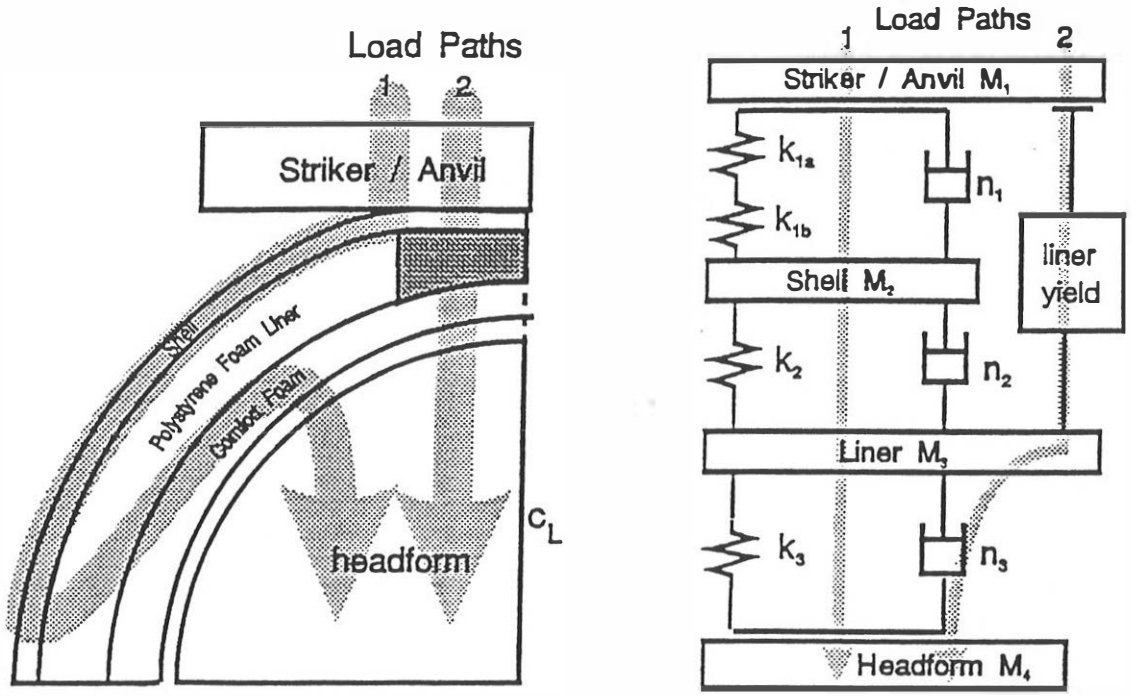

Fig. 1 (a) The load paths between a rigid flat surface (the road) and the head, (b) the equivalent mass, spring and damper model.

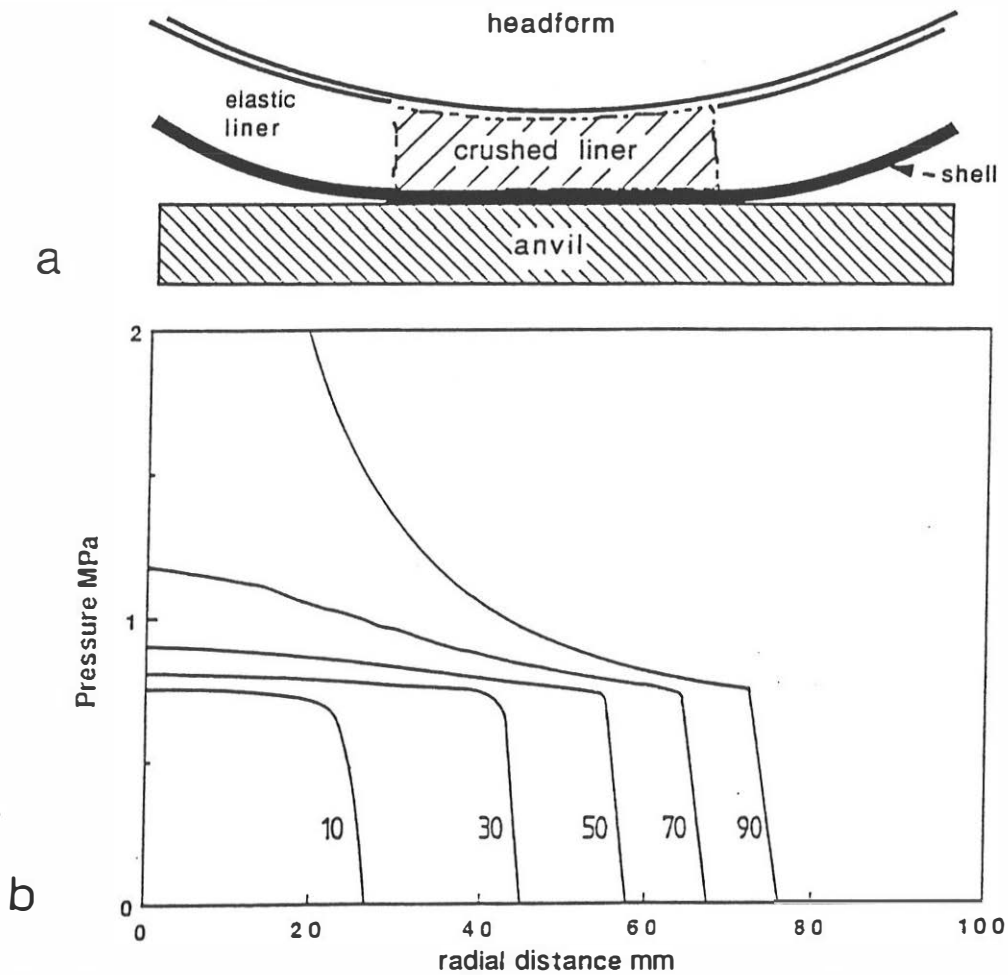

Fig. 2 (a)The assumed pattern of deformation near the impact site. The identical shapes of the headform and the liner interior mean that the headform cannot penetrate the liner from the inside.(b) the radial pressure distribution across a crushed density 56 kg m^{-3} density liner, for central liner strains of 10, 30, .. 90%, and a liner outer radius of 140 mm.hitting a flat anvil.

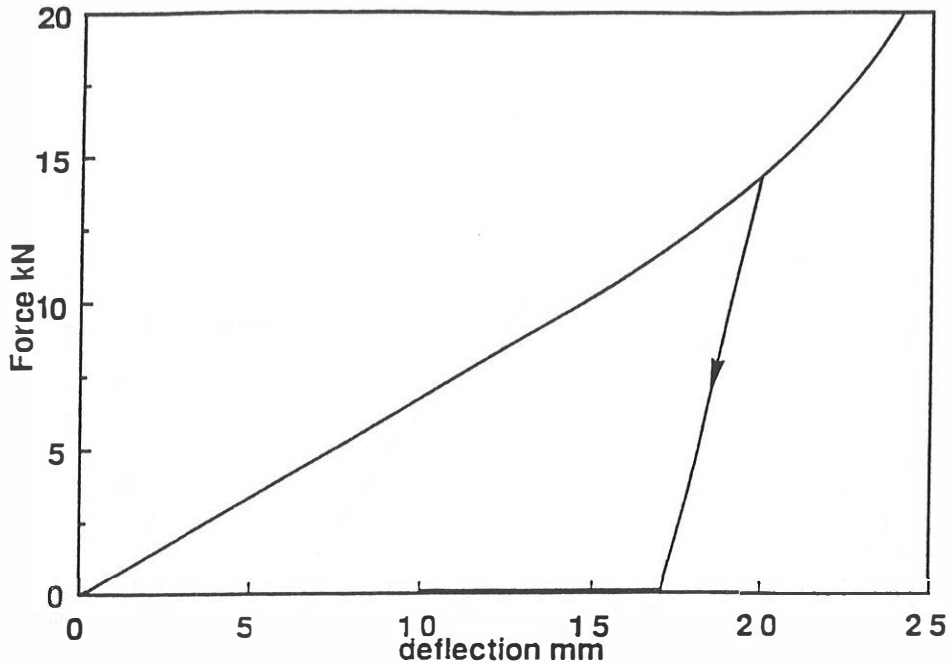

Fig. 3 Predicted contact force between a flat surface and a polystyrene foam liner of radius 140 mm,thickness 25 mm and density 56 kg m^{-3}, as a function of the central deflection, according to eqn.(5). An unloading path is shown.

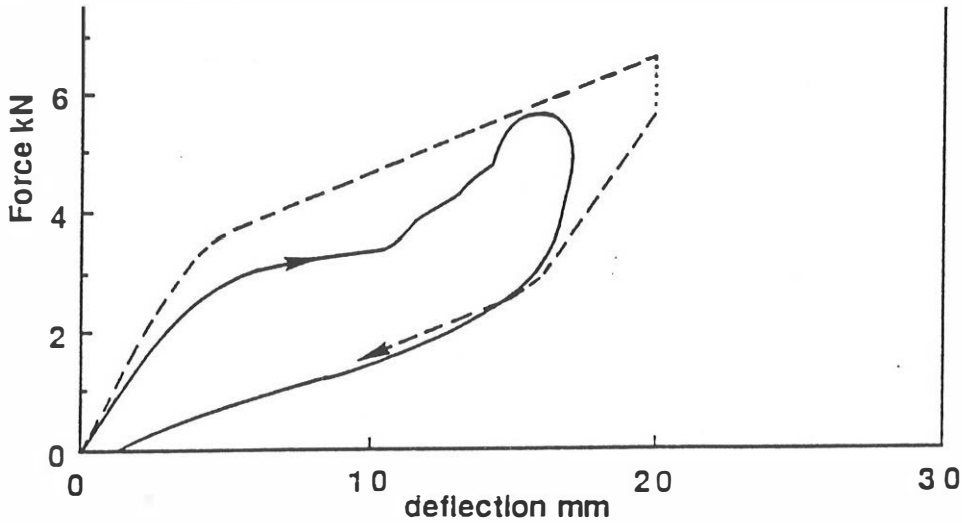

Fig. 4 The force-deformation trace for the ABS shell of a fullface helmet hit by a hemispherical striker.---- is the shell response used in the model k_{1a} = 700 , k_{1b} =200 N/mm after buckling at 3 kN; the loading velocity is taken as 5 m/s, and unloading at -5 m/s.

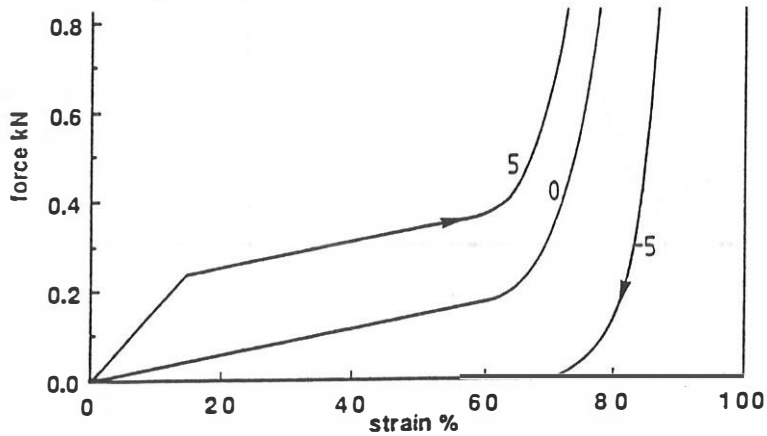

Fig. 5 The force-strain curve of a comfort foam, for a contact area of radius 75 mm, fitted with equation (9) with k_3 = 40 N/mm, n_3 = 40 Nsm^{-1}, for three velocities of compression(m s^{-1}).

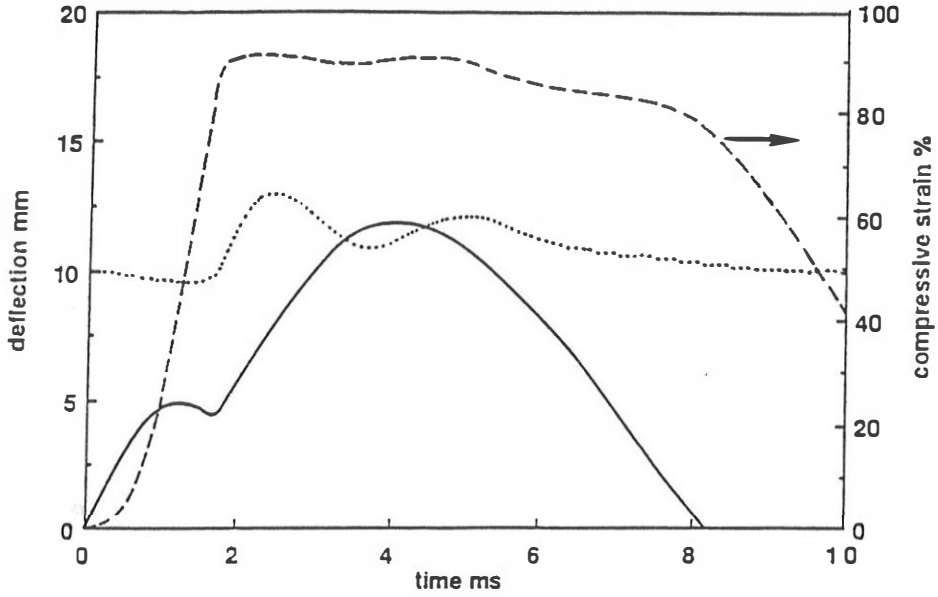

Fig. 6 Compression of the comfort foam ---- , liner crush —— and ..... elastic deflection of the liner(zero shifted up by 10 mm) versus time for an impact of a flat striker at 7.0 m s^{-1} on an ABS shell with a 56 kg m^{-3} density liner.

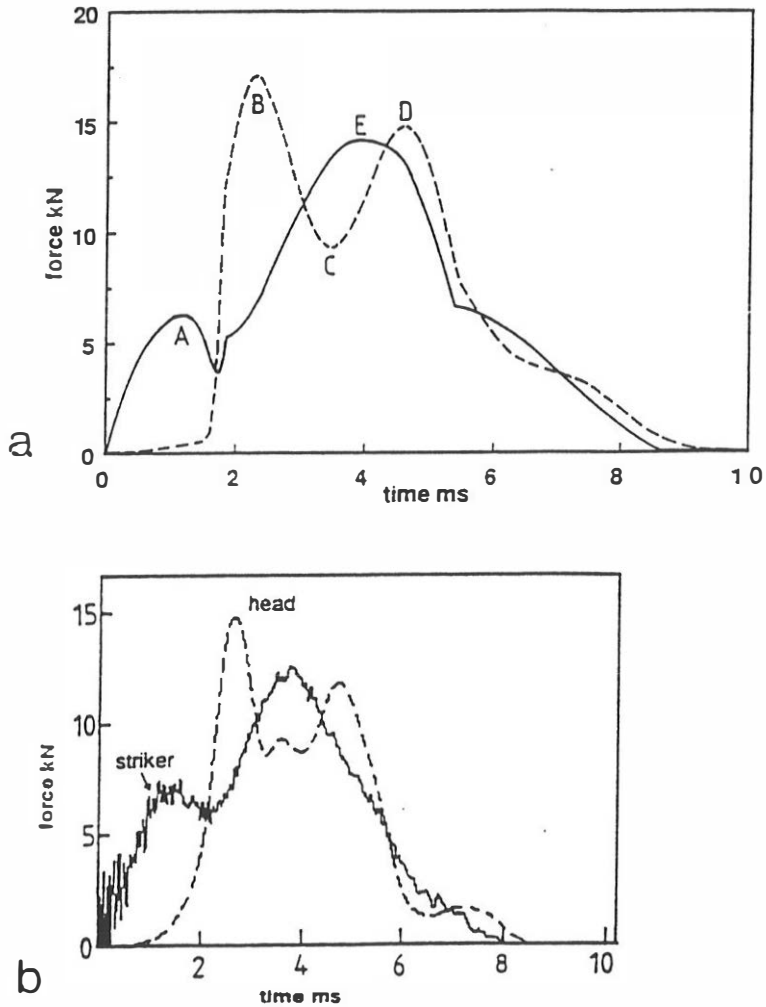

Fig. 7.(a) Predicted headform ---- and striker _____ force for the same conditions as Fig 6, (b) experimental data for a flat striker impact on the crown of a Jet style helmet at 7 m s^{-1}.

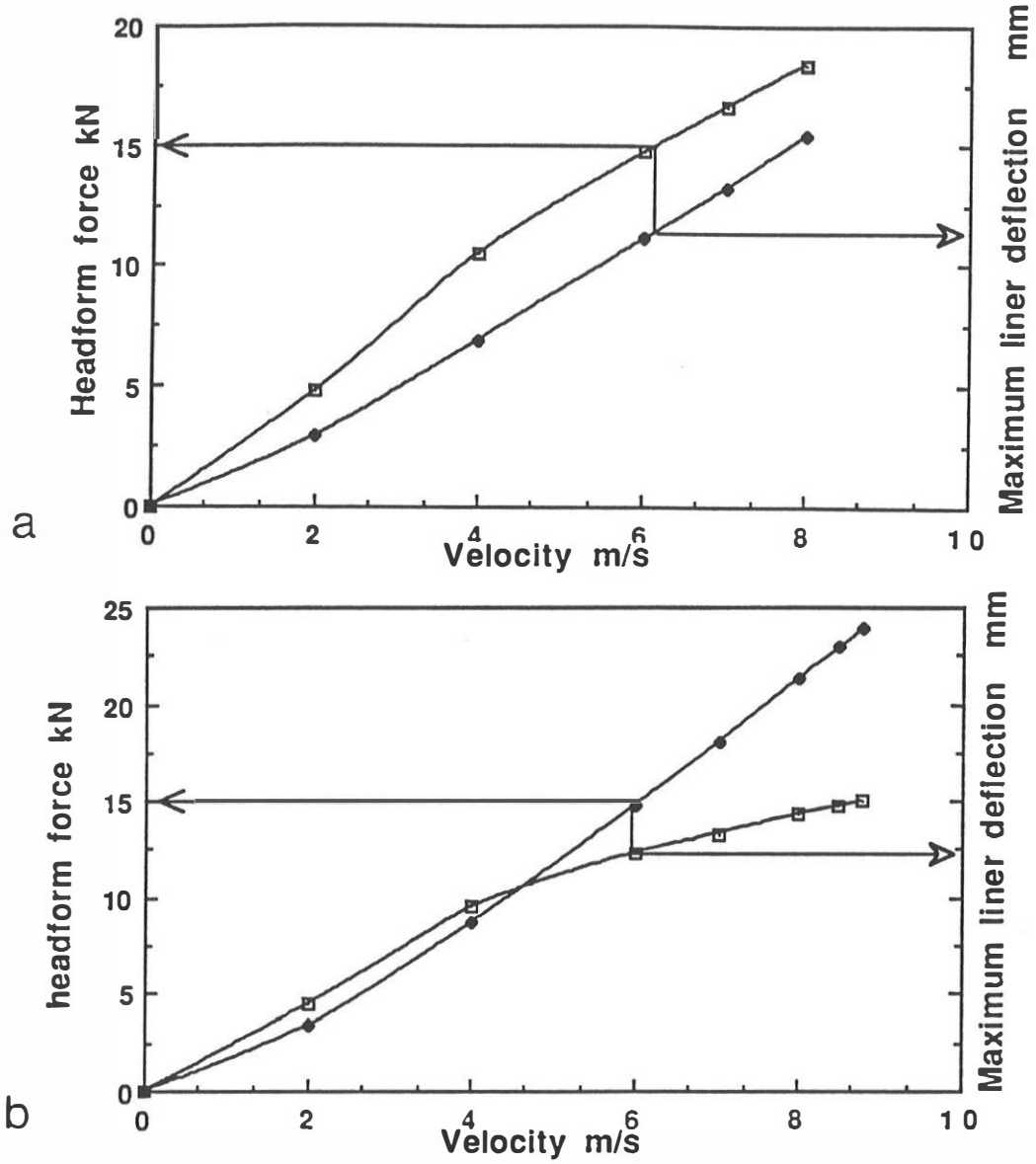

Fig. 8 Predicted peak headform force and maximum deformation of the liner foam versus impact velocity for an ABS shell & 56 kg m^{-3} liner on (a) flat, (b) hemispherical anvils. The impact site has radius of curvature 140 mm.

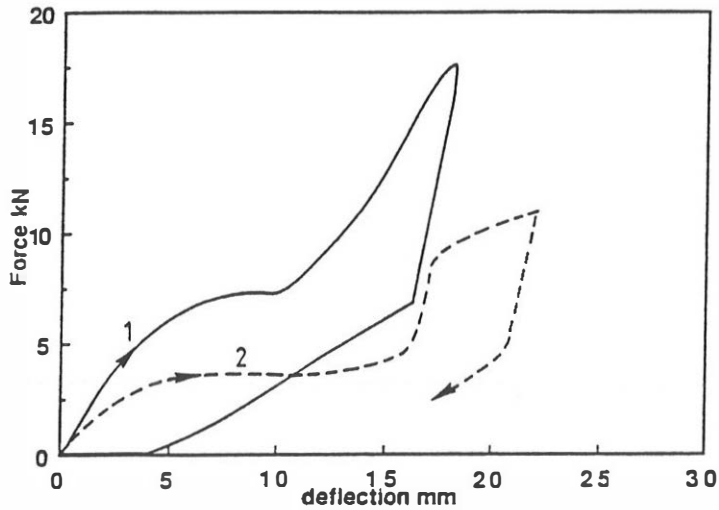

Fig 9. Simulated prEN 398 impacts for ABS shell & 56 kg m^{-3} liner, showing the anvil force versus the total foam deflection for —— the first impact at 7 ms^{-1} onto a flat anvil, ----- the second impact at 6 ms^{-1} onto a hemispherical anvil.